Octahedral Distortion and Displacement-Type Ferroelectricity with Switchable Photovoltaic Effect in a $3d^3$-Electron Perovskite System

B. W. Zhou,[1,2] J. Zhang,[1,2] X. B. Ye,[1,2] G. X. Liu,[1,2] X. Xu,[1,2] J. Wang,[3] Z. H. Liu,[1,2] L. Zhou,[1] Z. Y. Liao,[1,2] H. B. Yao,[1,2] S. Xu,[1,2] J. J. Shi,[1,2] X. Shen,[1] X. H. Yu,[1,2] Z. W. Hu,[4] H. J. Lin,[5] C. T. Chen,[5] X. G. Qiu,[1,2] C. Dong,[1,2] J. X. Zhang,[3] R. C. Yu,[1,2,6] P. Yu,[7] K. J. Jin,[1,2,6] Q. B. Meng,[1,2] and Y. W. Long[1,2,6,*]

[1]*Beijing National Laboratory for Condensed Matter Physics, Institute of Physics, Chinese Academy of Sciences, Beijing 100190, China*
[2]*School of Physics, University of Chinese Academy of Sciences, Beijing 100049, China*
[3]*Department of Physics, Beijing Normal University, Beijing 100875, China*
[4]*Max Planck Institute for Chemical Physics of Solids, Dresden 01187, Germany*
[5]*National Synchrotron Radiation Research Center, Hsinchu 30076, Taiwan*
[6]*Songshan Lake Materials Laboratory, Dongguan, Guangdong 523808, China*
[7]*State Key Laboratory of Low Dimensional Quantum Physics and Department of Physics, Tsinghua University, Beijing, 100084, China*

(Received 19 July 2022; revised 2 December 2022; accepted 14 March 2023; published 4 April 2023)

Because of the half-filled t_{2g}-electron configuration, the BO_6 octahedral distortion in a $3d^3$ perovskite system is usually very limited. In this Letter, a perovskitelike oxide $Hg_{0.75}Pb_{0.25}MnO_3$ (HPMO) with a $3d^3$ Mn^{4+} state was synthesized by using high pressure and high temperature methods. This compound exhibits an unusually large octahedral distortion enhanced by approximately 2 orders of magnitude compared with that observed in other $3d^3$ perovskite systems like $RCr^{3+}O_3$ (R = rare earth). Essentially different from centrosymmetric $HgMnO_3$ and $PbMnO_3$, the A-site doped HPMO presents a polar crystal structure with the space group $Ama2$ and a substantial spontaneous electric polarization (26.5 $\mu C/cm^2$ in theory) arising from the off-center displacements of A- and B-site ions. More interestingly, a prominent net photocurrent and switchable photovoltaic effect with a sustainable photoresponse were observed in the current polycrystalline HPMO. This Letter provides an exceptional d^3 material system which shows unusually large octahedral distortion and displacement-type ferroelectricity violating the "d^0-ness" rule.

DOI: 10.1103/PhysRevLett.130.146101

ABO_3 perovskite oxides have been receiving much attention due to their wide variety of interesting physical properties such as metal-insulator transition, high temperature superconductivity, colossal magnetoresistance, and multiferroic behavior [1–7]. The perovskite crystal structure is variable owing to the highly flexible BO_6 octahedral distortions (including different rotation and tilting), as initially described by Glazer and subsequently by Woodward [8–10]. Usually, a strong Jahn-Teller ion like Mn^{3+} or Cu^{2+} with a high-spin $3d^4$- or $3d^9$-electron configuration tends to induce a larger octahedral distortion and even cause orbital order as observed in manganese oxides [11–13]. In contrast, for a $3d^3$-electron system with a corner-sharing perovskite structure and half-filled t_{2g} orbitals like $R^{3+}Cr^{3+}O_3$ and $A^{2+}Mn^{4+}O_3$, the BO_6 octahedral distortion is relatively small. One may define a parameter $\Delta_d = \frac{1}{6}\sum_{n=1}^{6}[(d_n - \bar{d})/d]^2$ to describe the magnitude of the octahedral distortion [14]. Here, d_n and $\bar{d}$ denote a single and the average B—O bond length, respectively, in a BO_6 octahedron. As shown in Fig. 1, the values of Δ_d (unit: 10^{-4}) for the $3d^3$ perovskite family

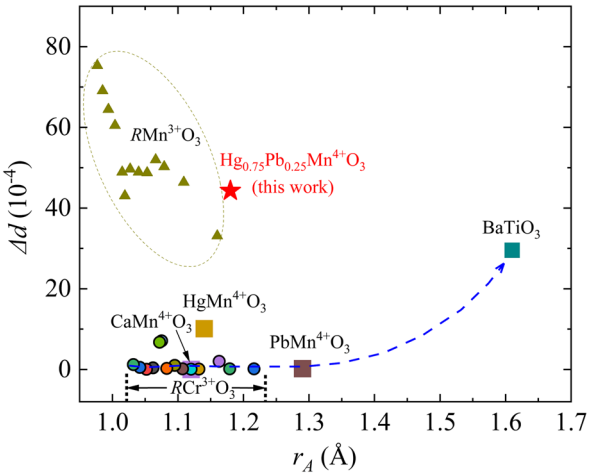

FIG. 1. Comparison of BO_6 octahedral distortion parameter (Δd) as a function of A-site ionic radius (r_A) for the non-Jahn-Teller Mn^{4+} and Cr^{3+} corner-sharing ABO_3 perovskites, the polarized $BaTiO_3$, and the Jahn-Teller active Mn^{3+} perovskites of $RMn^{3+}O_3$ at room temperature. The dashed curve is a guide.

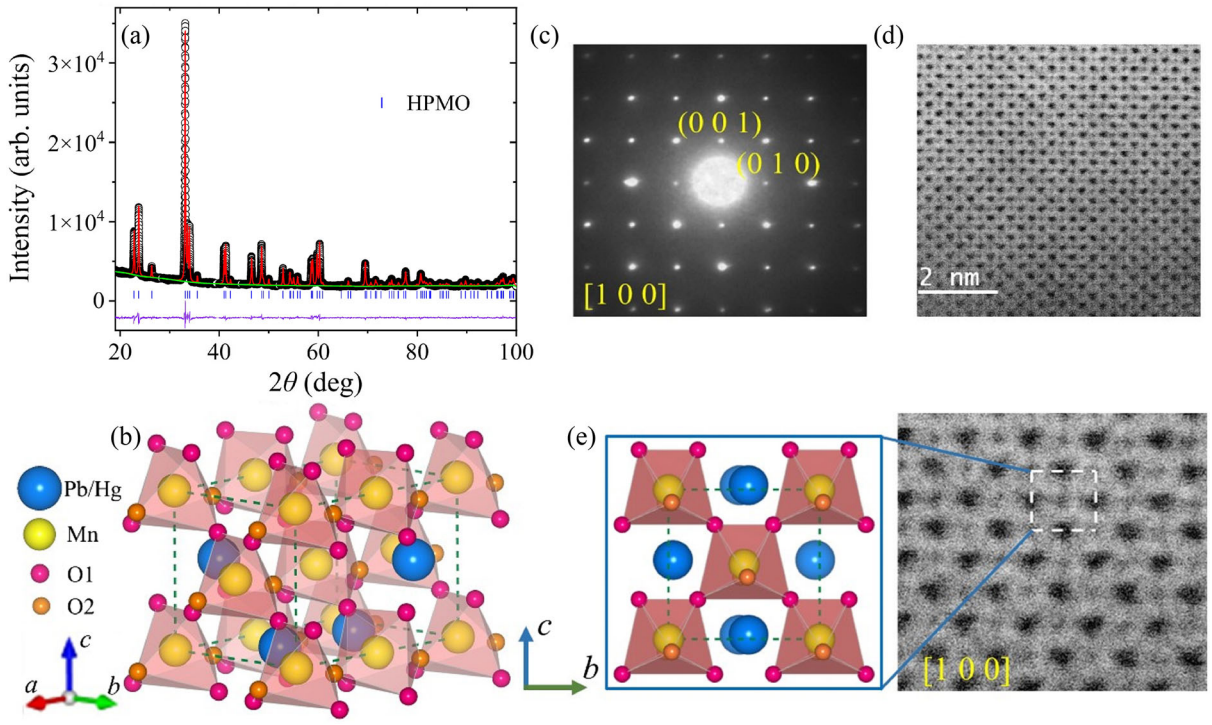

FIG. 2. (a) X-ray diffraction pattern and Rietveld refinement results of $Hg_{0.75}Pb_{0.25}MnO_3$ with polar space group $Ama2$ at room temperature. The observed (black circles), calculated (red line), background (green line), allowed Bragg reflections (blue ticks), and differences (purple line) are shown. A few weak diffraction peaks from unknown impurities were deleted from the pattern. (b) Schematic crystal structure of HPMO with heavily distorted MnO_6 octahedra. (c) The corresponding selected area electron diffraction pattern along the [100] zone axis. (d) The corresponding annular bright-field (ABF) image. (e) The enlarged ABF image (the white dashed box represents a unit cell).

$R^{3+}Cr^{3+}O_3$ are located in the range 0.1–1.2 except for Ho and Y [15–21]. For the $A^{4+}Mn^{4+}O_3$ family, the corner-sharing orthorhombic perovskite $CaMnO_3$ [22] and tetragonal $PbMnO_3$ [23] show comparable Δ_d values with those of $RCrO_3$. Although Hg^{2+} has a similar ionic radius to that of Ca^{2+}, the recently reported $HgMn^{4+}O_3$ with $P2_1/c$ space group displays a higher structure distortion with $\Delta_d = 10.1$ [24]. This observation suggests that the A-site electronic configuration may also play an important role for BO_6 octahedral distortion. Therefore, based on the highly distorted $HgMnO_3$, it can prove insightful to tune the structural distortion as well as the emergent physical properties by changing the A-site ionic size and electronic configuration.

In this study, the A-site doped $Hg_{0.75}Pb_{0.25}MnO_3$ (HPMO) with a $3d^3$ Mn^{4+} state was prepared using high-pressure (15 GPa) and high-temperature (1373 K) methods. Essentially different from the centrosymmetric $HgMnO_3$ ($P2_1/c$) and $PbMnO_3$ ($P4/mmm$) [23,24], the doped HPMO crystallizes to a polar crystal structure with off-center displacements contributed by both A- and B-site cations, regardless of the "d^0-ness" rule [25]. Unexpectedly, HPMO shows an unusually large octahedral distortion with the value of Δ_d as large as 44.3, which is comparable to those of the Jahn-Teller active perovskite systems like $R^{3+}Mn^{3+}O_3$ [26–29] (see Fig. 1). Moreover, a switchable ferroelectric photovoltaic effect [30–32] is found to occur, suggesting promising applications for this polycrystalline material at room temperature.

Detailed experimental methods used in this Letter are described in the Supplemental Material [33]. The x-ray diffraction (XRD) pattern and Rietveld refinement results of HPMO performed at room temperature are shown in Fig. 2(a). HPMO displays essentially different diffraction peaks from those of $HgMnO_3$ and $PbMnO_3$, indicating the presence of a new crystal structure. We first searched for ABO_3-type isostructural references to resolve the crystal structure. However, there are no satisfactory isostructural models that display XRD features similar to those of HPMO. Therefore, based on the EXPO2014 program [45], we applied a direct method to find primary structural parameters, including possible space groups, lattice constants, and atomic positions; Rietveld refinements were further performed according to the direct-method information. The most reliable structural model was then determined by comparing the goodness-of-fit parameters such as R_p and R_{wp}, and judging the rationality of the fitted bond lengths and angles, etc. Through this process, we found that the XRD data of HPMO can be best fitted based on a polar orthorhombic space group $Ama2$ (no. 40) with satisfactory

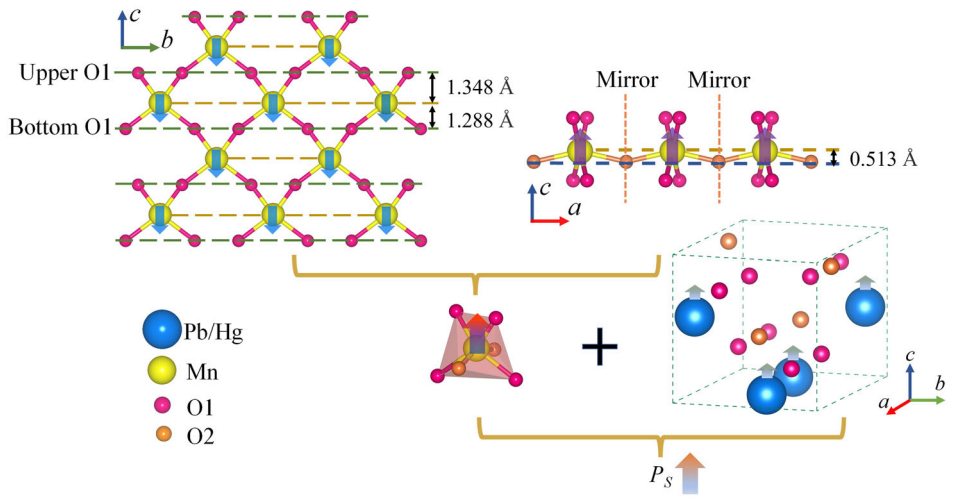

FIG. 3. Diagram of the origin of spontaneous polarization (P_S) induced by cation displacements in HPMO. The arrows indicate the directions of P_S. The net electric polarization generated by *A*- and *B*-site displacements are both along the crystal *c*-axis direction.

factors $R_p = 2.21\%$ and $R_{wp} = 2.93\%$. In this polar structure, there is a single Wyckoff position 4*b* (0.25, *y*, *z*) for Hg/Pb, and 4*a* (0, 0, z) for Mn, while there are two distinct positions for the ligand O atoms, i.e., 8*c* (*x*, *y*, *z*) for O1 and 4*b* (0.25, *y*, *z*) for O2. Figure 2(b) shows a schematic of the HPMO crystal structure with a highly distorted MnO_6 octahedral network. The primitive cell comprises four formula units ($Z = 4$) with corner-sharing MnO_6 octahedra, forming a perovskite-type construction. To further confirm the proposed polar structure, selected area electron diffraction (SAED) and annular bright-field (ABF) imaging were carried out. Figures 2(c) and 2(d) indicate the corresponding SAED pattern and ABF image along the [100] zone axis, respectively. Based on the contrast analysis shown in Fig. 2(e), the positions of atomic columns for elements (Hg/Pb, Mn, and O) are found to perfectly match the theoretical model obtained from the XRD refinement results. Moreover, the determination of such a polar structure agrees well with the observed second harmonic generation (SHG) and ferroelectricity shown later.

Supplemental Material Table S1 [33] lists some refined crystallographic parameters including the atomic positions, bond lengths, Mn—O—Mn bond angles, etc. There are two kinds of Mn—O—Mn bond angles, 155.1°, and 149.1°. In the *Pnma* (*no.* 62) orthorhombic perovskite $CaMnO_3$ [22], the average Mn—O—Mn bond angle (147.2°) is somewhat smaller than that of the current HPMO (153.1°), as expected from the reduced *A*-site ionic size (1.18 Å in HPMO as opposed to 1.12 Å in $CaMnO_3$). According to the refined atomic positions, the cation-displacement-induced spontaneous ferroelectric polarization (P_S) can be analyzed. As illustrated in Fig. 3, if the Mn and O1 atoms are projected onto the *bc* plane, the Mn layer appears to deviate from the upper oxygen layer by 1.348 Å. However, the Mn layer deviates by 1.288 Å from the bottom oxygen layer along the *c* axis, suggesting the presence of a net displacement of Mn with respect to O1 in the opposite direction along the *c* axis. In the *Ama*2 symmetry, mirror planes exist that are perpendicular to the *a* axis. As shown in Fig. 3, the Mn layer has a larger *c* axis off-centering by 0.513 Å relative to the O2 atoms arranged along the *a* axis. In total, the electric polarization direction caused by the Mn-displacement in MnO_6 octahedra is toward the *c* axis. Owing to its $3d^3$ electronic configuration, the current HPMO provides a rare example that violates the so-called "d^0-ness" rule for displacement-type ferroelectrics. In addition, based on the crystal symmetry analysis, it can be determined that the electric polarization arising from the *A*-site Pb/Hg displacements is also along the *c* axis. The total polarization calculated using the point charge model is 26.5 $\mu C/cm^2$ along the crystal *c*-axis direction. Such a large P_S value is comparable to the values observed in other displacement-type ferroelectrics, such as $BaTiO_3$ [46] and $BiFeO_3$ [47].

Based on the refined Mn—O bond lengths, the bond valence sum calculations (+3.75 as seen in Table S1 [33]) suggest the formation of an Mn^{4+} valence state in HPMO, as revealed by x-ray absorption spectroscopy [48,49] shown in Supplemental Material Fig. S1 [33]. In contrast to other reported $3d^3$ perovskite systems, the *B*—O bond lengths of the current HPMO vary substantially in a single MnO_6 octahedron in the range 1.77–2.06 Å, which indicates the presence of an unusually large octahedral distortion. Based on the octahedral distortion parameter Δ_d mentioned above, the value of Δ_d for HPMO is calculated to be as high as 44.3, which is substantially higher than those observed in other $3d^3$ corner-sharing perovskite oxides by approximately 2 orders of magnitude, and comparable with most Jahn-Teller active Mn^{3+} systems in the $RMnO_3$ perovskite family, as summarized in Fig. 1. As is well known, no remarkable octahedral distortion is

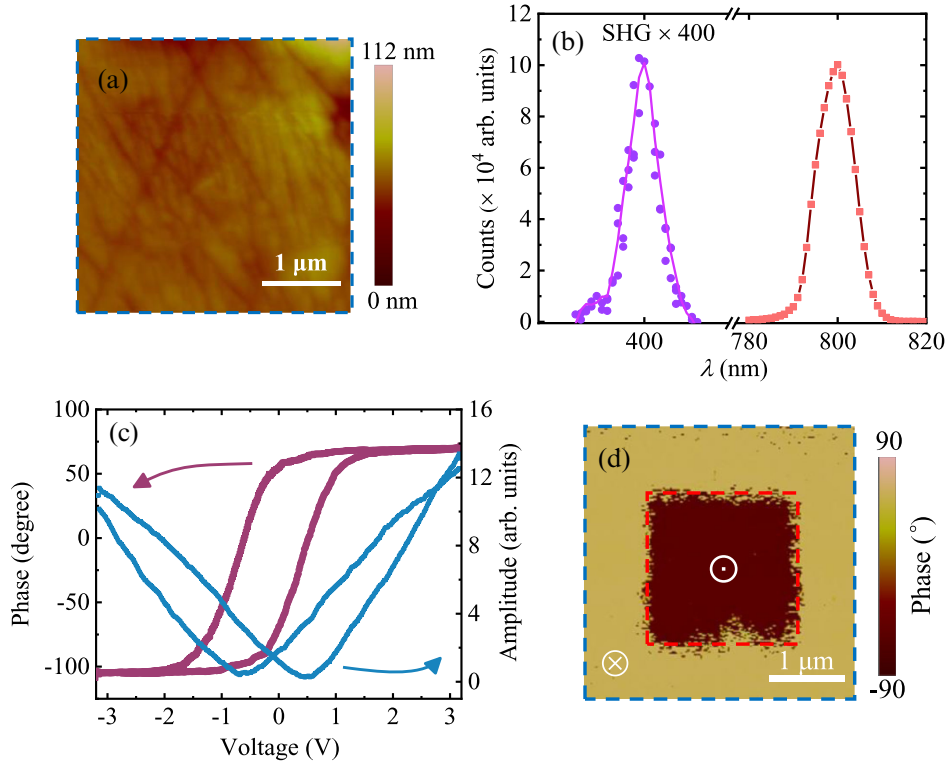

FIG. 4. (a) Surface topography of HPMO by atomic force microscopy. (b) Second harmonic generation (SHG) signal (400 nm) and fundamental wavelength peak (800 nm) of the spectroscopic data at 300 K. (c) Piezoresponse phase hysteresis loop (purple) and amplitude butterfly (blue) of HPMO. (d) Out-of-plane piezoresponse force microscopy images after probe bias switching by two-step box-in-box electric poling. The bright and dark contrasts indicate the downward and upward polarization states, respectively.

expected to occur in the non-Jahn-Teller Mn^{4+} ion due to the half-filled t_{2g} orbitals. The unusually large structure distortion observed in HPMO is likely related to the polarized crystal structure. For example, the tetragonally distorted ferroelectric $BaTiO_3$ also displays a considerable Δ_d up to 29.6, as presented in Fig. 1 [50]. In addition, some stresses may exist in the quenched HPMO synthesized at an extremely high pressure (15 GPa), which may also favor the distorted structure. As shown in Supplemental Material Fig. S2 [33], the nonpolar $HgMnO_3$ [24] exhibits the largest variation for the A—O distance probably due to the small ionic size of Hg^{2+}, while the nonpolar $PbMnO_3$ [23] shows the lowest variation. In comparison, the change of A—O distance for the polar HPMO with the net Hg/Pb displacement along the crystal c axis is located between $HgMnO_3$ and $PbMnO_3$, which is very similar to that of the polar $PbTiO_3$ [42]. In our experiments on the solid solution of $Hg_{1-x}Pb_xMnO_3$, only the composition with $0.2 \leq x \leq 0.3$ shows a polar structure (not shown here). Moreover, the Mn—O distance in the polar HPMO displays much greater fluctuation than that of the nonpolar $HgMnO_3$ and $PbMnO_3$ (Supplemental Material Fig. S3 [33]). It appears that a moderate A-site size and lone electronic pairs must be delicately balanced to induce a polarized structure with sharply enhanced octahedral distortion in the $Hg_{1-x}Pb_xMnO_3$ family.

Room-temperature SHG and piezoresponse force microscopy (PFM) were performed on polycrystalline HPMO to confirm the determined polar structure. After high pressure treatment, a hard piece was carefully polished using a diamond sandpaper (1.0 μm particle size) to a diameter of 1.5 mm and thickness of 0.1 mm for SHG and PFM measurements. Figure 4(a) shows the topography of the polished surface. Measurements were made using atomic force microscopy and indicated the formation of an approximately level plane. When fundamental incident light with a wavelength of 800 nm was applied to shine on the polished surface, a clear peak centered at 400 nm was observed, confirming the occurrence of the SHG signal, as shown in Fig. 4(b). Moreover, applying electric fields can significantly enhance the SHG signal (see Supplemental Material Fig. S4 [33]), which is consistent with the noncentrosymmetric polar structure of HPMO. As presented in Fig. 4(c), a PFM hysteretic phase loop and a typical butterfly curve of the amplitude loop with a probe bias voltage in the range from −3.2 to +3.2 V were observed, suggesting that ferroelectricity is expected to occur in HPMO. As shown in Fig. 4(d), polarization switching of the domains was conducted by two-step electric poling. The domain pattern in the blue dotted box was first switched by a positive probe bias voltage to create an out-of-plane downward polarization. Second, a smaller box

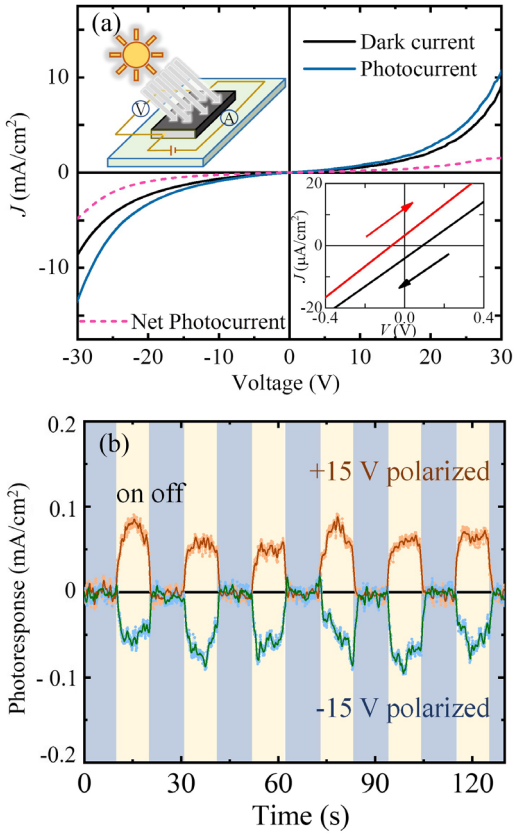

FIG. 5. (a) Electric current density (J) and voltage (V) characteristics measured from −30 to +30 V for Ag/HPMO/Ag device. The net photocurrent is the photocurrent under illumination subtracted by dark current. The upper left inset shows a setup diagram for the photovoltaic device. The bottom right inset shows $J-V$ curves under poling and illumination in the low bias region. The arrows indicate poling direction reversion. (b) Reproducible photocurrent response with periodic dependent on-off switching under +/−15 V polarized electric fields.

area (the red dotted box) in the center was rewritten using a negative probe bias voltage to flip the polarization to the upward direction. Two-step electric poling was achieved to further confirm the switchable polarization of ferroelectric domains and written or erased controllability by electric fields. Note that, due to the leakage effect, one cannot detect macroscopic ferroelectric hysteresis loops in the bulk HPMO sample.

Optical absorption measurement shows that HPMO has a direct band gap of 2.25 eV (refer to Supplemental Material Fig. S5 [33]), which is in the range of visible light. Considering the ferroelectricity and moderate band gap of HPMO, a ferroelectric photovoltaic effect may occur. A metal-ferroelectric-metal sandwich structure, Ag/HPMO/Ag, was designed as the device architecture for the photovoltaic test as shown in the upper inset of Fig. 5(a). Usually, the ferroelectric photovoltaic effect is observed to have a diodelike rectification behavior due to the high insulation characteristics and the Schottky effect within ferroelectric devices such as $BiFeO_3$-based devices [51–53]. However, as shown in Fig. 5(a), HPMO presents a high dark current from −30 to +30 V, possibly originating from the electromigration of grain boundaries in polycrystalline or interfacial oxygen vacancies [54,55]. Under white light illumination, an obvious net photocurrent was obtained, depending on the electric fields. Although the zero bias short-circuit photocurrent is small as shown in the bottom inset of Fig. 5(a), the photovoltage is switchable by reversing the poling electric field. The excited carriers can be simultaneously stimulated by light switching and polarized electric fields to maintain a repeatable photocurrent. The time-dependent photoresponse was thus acquired under +/−15 V polarized electric fields, as shown in Fig. 5(b). The photoresponse means the net photocurrent under switching repetition with "on/off" white light incidence, and the photocurrent direction were also tuned by electric field direction reversion. The photocurrent was clearly observable in the polycrystalline-based Ag/HPMO/Ag device under illumination and external electric fields, although the response without applying a poling electric field is small due to the leakage effect.

In summary, a new ferroelectric perovskite-type oxide HPMO was prepared using high-pressure (15 GPa) and high-temperature (1373 K) methods. Distinct from centrosymmetric $HgMnO_3$ and $PbMnO_3$, the A-site doped HPMO shows a polar crystal structure with space group $Ama2$. An unusually large octahedral distortion is found to occur in the current HPMO compared to other corner-sharing $3d^3$-electron perovskite systems with half-filled t_{2g} orbitals by 2 orders of magnitude. A substantial displacement-type ferroelectricity was illustrated based on a detailed structural analysis regardless of the "d^0-ness" rule. The room-temperature polar structure and ferroelectricity were further confirmed by SHG and PFM measurements. The optical absorption and photoluminescence spectra indicate a moderate direct band gap within the visible light region. A net photocurrent and switchable photovoltaic effect were observed based on a simple device comprised of Ag/HPMO/Ag. The polycrystalline ferroelectric compound HPMO with sharply enhanced octahedral distortion provides a promising candidate for solar cell functionalities and optoelectronic devices.

The authors thank Z. G. Yi and C. Chen for helpful discussion. This work was supported by the National Key R&D Program of China (Grant No. 2021YFA1400300, and No. 2018YFA0305700), the Beijing Natural Science Foundation (Grant No. Z200007), the National Natural Science Foundation of China (Grants No. 11934017, No. 12261131499, No. 11921004, No. 11904392, and No. 11721404), and the Chinese Academy of Sciences (Grant No. XDB33000000). We acknowledge support from the Max Planck-POSTECH-Hsinchu Center for Complex Phase Materials.

*ywlong@iphy.ac.cn

[1] M. Imada, A. Fujimori, and Y. Tokura, Rev. Mod. Phys. **70**, 1039 (1998).
[2] A. W. Sleight, J. L. Gillson, and P. E. Bierstedt, Solid State Commun. **88**, 841 (1993).
[3] P. Schiffer, A. P. Ramirez, W. Bao, and S. W. Cheong, Phys. Rev. Lett. **75**, 3336 (1995).
[4] S. Yamada, N. Abe, H. Sagayama, K. Ogawa, T. Yamagami, and T. Arima, Phys. Rev. Lett. **123**, 126602 (2019).
[5] J. S. Zhou and J. B. Goodenough, Phys. Rev. Lett. **96**, 247202 (2006).
[6] J. Wang *et al.*, Science **299**, 1719 (2003).
[7] M. Fiebig, T. Lottermoser, D. Fröhlich, A. V. Goltsev, and R. V. Pisarev, Nature (London) **419**, 818 (2002).
[8] A. Glazer, Acta Crystallogr. Sect. B **28**, 3384 (1972).
[9] P. Woodward, Acta Crystallogr. Sect. B **53**, 32 (1997).
[10] P. Woodward, Acta Crystallogr. Sect. B **53**, 44 (1997).
[11] E. Dagotto, T. Hotta, and A. Moreo, Phys. Rep. **344**, 1 (2001).
[12] T. Mizokawa and A. Fujimori, Phys. Rev. B **56**, R493 (1997).
[13] Y. Tokura and N. Nagaosa, Science **288**, 462 (2000).
[14] J. S. Zhou and J. B. Goodenough, Phys. Rev. Lett. **94**, 065501 (2005).
[15] K. D. Singh, R. Pandit, and R. Kumar, Solid State Sci. **85**, 70 (2018).
[16] V. S. Bhadram, D. Swain, R. Dhanya, M. Polentarutti, A. Sundaresan, and C. Narayana, Mater. Res. Express **1**, 026111 (2014).
[17] B. B. Dash and S. Ravi, J. Magn. Magn. Mater. **405**, 209 (2016).
[18] Y. Sharma, S. Sahoo, W. Perez, S. Mukherjee, R. Gupta, A. Garg, R. Chatterjee, and R. S. Katiyar, J. Appl. Phys. **115**, 183907 (2014).
[19] K. Tsushima, I. Takemura, and S. Osaka, Solid State Commun. **7**, 71 (1969).
[20] K. Yoshii and A. Nakamura, J. Solid State Chem. **155**, 447 (2000).
[21] L. Wang, G. H. Rao, X. Zhang, L. L. Zhang, S. W. Wang, and Q. R. Yao, Ceram. Int. **42**, 10171 (2016).
[22] I. O. Troyanchuk, S. N. Pastushonok, O. A. Novitskii, and V. I. Pavlov, J. Magn. Magn. Mater. **124**, 55 (1993).
[23] X. Li *et al.*, Chem. Mater. **33**, 92 (2021).
[24] B. Zhou *et al.*, Inorg. Chem. **59**, 3887 (2020).
[25] D. Y. Cho *et al.*, Phys. Rev. Lett. **98**, 217601 (2007).
[26] J. Rodríguez-Carvajal, M. Hennion, F. Moussa, A. H. Moudden, L. Pinsard, and A. Revcolevschi, Phys. Rev. B **57**, R3189(R) (1998).
[27] T. Mori, N. Kamegashira, K. Aoki, T. Shishido, and T. Fukuda, Mater. Lett. **54**, 238 (2002).
[28] J. A. Alonso, M. J. Martínez-Lope, M. T. Casais, and M. T. Fernández-Díaz, Inorg. Chem. **39**, 917 (2000).
[29] M. Tachibana, T. Shimoyama, H. Kawaji, T. Atake, and E. Takayama-Muromachi, Phys. Rev. B **75**, 144425 (2007).
[30] D. Cao, C. Wang, F. Zheng, W. Dong, L. Fang, and M. Shen, Nano Lett. **12**, 2803 (2012).
[31] C. Paillard, X. Bai, I. C. Infante, M. Guennou, G. Geneste, M. Alexe, J. Kreisel, and B. Dkhil, Adv. Mater. **28**, 5153 (2016).
[32] H. Huang, Nat. Photonics **4**, 134 (2010).
[33] See Supplemental Material at http://link.aps.org/supplemental/10.1103/PhysRevLett.130.146101, which includes Refs. [23,24,33–44], for experimental methods, refined crystallographic parameters, x-ray absorption spectra of Mn-$L_{2,3}$ edges, comparison of the *A*-site Hg/Pb—O bond lengths and *B*-site Mn—O bond lengths, SHG signal measured at different voltages, and optical absorption spectra of HPMO at room temperature.
[34] J. Rodríguez-Carvajal, Physica (Amsterdam) **192B**, 55 (1993).
[35] J. X. Zhang *et al.*, Phys. Rev. Lett. **107**, 147602 (2011).
[36] R. Zhao, K. Jin, H. Guo, H. Lu, and G. Yang, Sci. China Phys. Mech. **56**, 2370 (2013).
[37] J. S. Wang, K.-j. Jin, J.-x. Gu, Q. Wan, H.-b. Yao, and G.-z. Yang, Sci. Rep. **7**, 9051 (2017).
[38] C. C. Homes, M. Reedyk, D. A. Cradles, and T. Timusk, Appl. Opt. **32**, 2976 (1993).
[39] I. D. Brown and D. Altermatt, Acta Crystallogr. Sect. B **41**, 244 (1985).
[40] T. Burnus *et al.*, Phys. Rev. B **77**, 125124 (2008).
[41] S. Qin, Y.-Y. Chin, B. Zhou, Z. Liu, X. Ye, J. Guo, G. Liu, C.-T. Chen, Z. Hu, and Y. Long, Inorg. Chem. **60**, 16308 (2021).
[42] K. Shahzad, M. Nasir Khan, G. Shabbir, and J. Bashir, Ferroelectrics **414**, 155 (2011).
[43] A. Ibrahim and S. K. J. Al-Ani, Czech. J. Phys. **44**, 785 (1994).
[44] S. Seth, T. Ahmed, A. De, and A. Samanta, ACS Energy Lett. **4**, 1610 (2019).
[45] A. Altomare, C. Cuocci, C. Giacovazzo, A. Moliterni, R. Rizzi, N. Corriero, and A. Falcicchio, J. Appl. Crystallogr. **46**, 1231 (2013).
[46] W. J. Merz, Phys. Rev. **91**, 513 (1953).
[47] K. Y. Yun, M. Noda, and M. Okuyama, Appl. Phys. Lett. **83**, 3981 (2003).
[48] C. Mitra, Z. Hu, P. Raychaudhuri, S. Wirth, S. I. Csiszar, H. H. Hsieh, H.-J. Lin, C. T. Chen, and L. H. Tjeng, Phys. Rev. B **67**, 092404 (2003).
[49] M. A. Hossain *et al.*, Phys. Rev. Lett. **101**, 016404 (2008).
[50] S. Miyake and R. Ueda, J. Phys. Soc. Jpn. **2**, 93 (1947).
[51] J. Xing, E.-J. Guo, J. Dong, H. Hao, Z. Zheng, and C. Zhao, Appl. Phys. Lett. **106**, 033504 (2015).
[52] S. Y. Yang *et al.*, Appl. Phys. Lett. **95**, 062909 (2009).
[53] T. Choi, S. Lee, Y. J. Choi, V. Kiryukhin, and S. W. Cheong, Science **324**, 63 (2009).
[54] A. J. Hauser, J. Zhang, L. Mier, R. A. Ricciardo, P. M. Woodward, T. L. Gustafson, L. J. Brillson, and F. Y. Yang, Appl. Phys. Lett. **92**, 222901 (2008).
[55] Y. Yan *et al.*, Physica (Amsterdam) **401-402B**, 25 (2007).